Aberration correction in coherence imaging microscopy

D. Weigel, A. Kießling, R. Kowarschik
Institute of Applied Optics, Abbe Center of Photonics,
Center for Medical Optics and Photonics
Friedrich Schiller University Jena

FSU Jena

institute iao of applied optics

Introduction

Coherence imaging microscopy enables a high-resolution optical microscopy with an infinite depth of field [P31]. For that purpose, the complex coherence function Γ in the exit pupil (EP) of the microscope objective (MO) is determined, from which the spatially incoherent object structure is reconstructed [1]. Using an image inverting interferometer (III), it is possible to measure Γ with a high spatial resolution [2]. Phase aberrations caused by the imaging optics or the specimen itself influence only the phase of Γ. As a consequence, after measuring Γ a purely numerical correction of these aberrations is possible [3].
As we will show, the presented setup has the advantage that aberrations which are symmetric to the optical axis do not disturb the reconstruction of object structures. Moreover, we demonstrate that it is possible to determine remaining wavefront errors by a reference measurement and to correct them numerically.

Theory

The basic principles of coherence imaging microscopy are discussed on poster P31. Here the derivation is expanded to investigate the influence of phase aberrations. Using an III, Γ can be written as the time average of the amplitude distribution U_P in the EP of the MO MO multiplied with its spatially inverted copy (Eq.1). By the definition of U_P [P31], the pupil function $P(\vec{r}/R)$ can be written in front of the average (Eq.2). Here, U_L denotes the amplitude distribution in the entrance pupil. Using a generalized pupil function (Eq.3), it is obvious that only aberrations satisfying Eq.4 influence the phase of Γ. Therefore, if a conventional circular pupil is assumed, Γ can be written as Eq.5.
Due to the fact that phase aberrations only influence the phase of Γ, it is possible to correct the effective aberrations purely numerical by multiplying the measured Γ by the inverse aberration function. As a result, Γ can be treated as diffraction-limited (Eq.6).
To obtain the aberration function $\Delta\phi$, it is necessary to image a defined reference wavefront through the optical system, including the III, onto the detector. A spherical wave is most appropriate for that purpose as it is easy to realize and to analyze.

$$(1)\quad \Gamma(\Delta\vec{r}) = \left\langle U_P(\vec{r},t)\cdot U_P^*(-\vec{r},t)\right\rangle_t$$

$$(2)\quad \Gamma(\Delta\vec{r}) = P(\vec{r}/R)P^*(-\vec{r}/R)\cdot\left\langle U_L(\vec{r},t)\cdot U_L^*(-\vec{r},t)\right\rangle_t$$

$$(3)\quad P(\vec{r}/R) = p(\vec{r}/R)\cdot \mathrm{e}\left(i\,\frac{2\pi}{\lambda}\,\phi(\vec{r})\right)$$

$$(4)\quad \Delta\phi(\vec{r}) = \phi(\vec{r}) - \phi(-\vec{r})$$

$$(5)\quad \Gamma(\Delta\vec{r}) = p(\vec{r}/R)\cdot \mathrm{e}\left(i\,\frac{2\pi}{\lambda}\,\Delta\phi(\vec{r})\right) \times \left\langle U_L(\vec{r},t)\cdot U_L^*(-\vec{r},t)\right\rangle$$

$$(6)\quad \Gamma(\Delta\vec{r}) = p(\vec{r}/R)\cdot\left\langle U_L(\vec{r},t)\cdot U_L^*(-\vec{r},t)\right\rangle_t = p(\vec{r}/R)\cdot\mathcal{F}\left\{I(\vec{\rho})\right\}$$

Setup

Fig.1

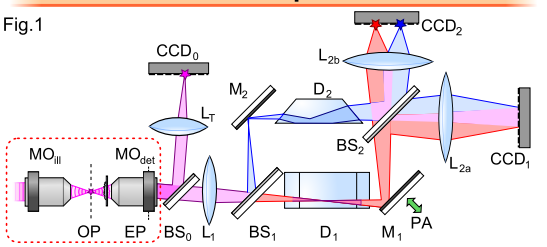

Sketch of the setup. The exit pupil (EP) of the microscope objective MO_{det} (NA = 0.07, 2.5x) is imaged through the III onto the detector CCD_1 by the lenses L_1 and L_{2a}. The Dove prisms D_1 and D_2 are rotated by 90° to each other, leading to the required image inversion. The piezo-actuator PA is used to adjust the optical path difference between the two arms of the III. With the help of the lens L_{2b} and CCD_2, the conventional image can be taken, containing the aberrations of the whole optical system (MO_{det} + III). Here, CCD_0 is used to capture control images and to adjust the system.

Fig.2

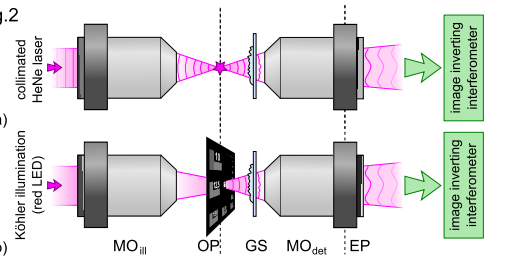

Magnified view of the red dashed part of Fig. 1. A transparent adhesive film on a glass slide (GS) produces additional wavefront errors. By positioning the slide, different random aberrations can be generated. (a) Shows the determination of the aberrations with the help of a focused helium neon (HeNe) laser beam. After measuring the aberrations, the test chart was imaged. Due to the required spatially incoherent illumination, a Köhler illumination was used. As the source of light, a red LED ($\lambda \approx 633$ nm) was applied.

Fig.3

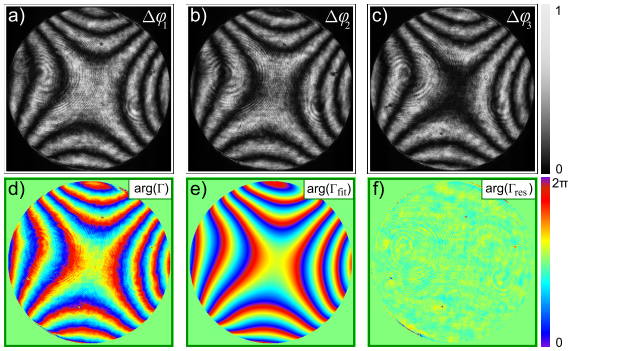

To determine wavefront errors, a HeNe laser beam was focused into the OP of MO_{det}. Hence, three interferograms are sufficient to calculate the complex valued Γ (a-c). Due to image noise and coherent artifacts, fine structures disturb the phase of Γ (d). To reduce these disturbances, the phase is decomposed into Zernike polynomials up to the 10th order. As a result, a smooth phase distribution can be obtained (e). The residual errors (f), being the difference of d) and e), can be interpreted as a measure of the quality of the Zernike polynomial fit. Here, all relevant aberrations could be considered by the fit and only the artifacts remain in f).

Fig.4

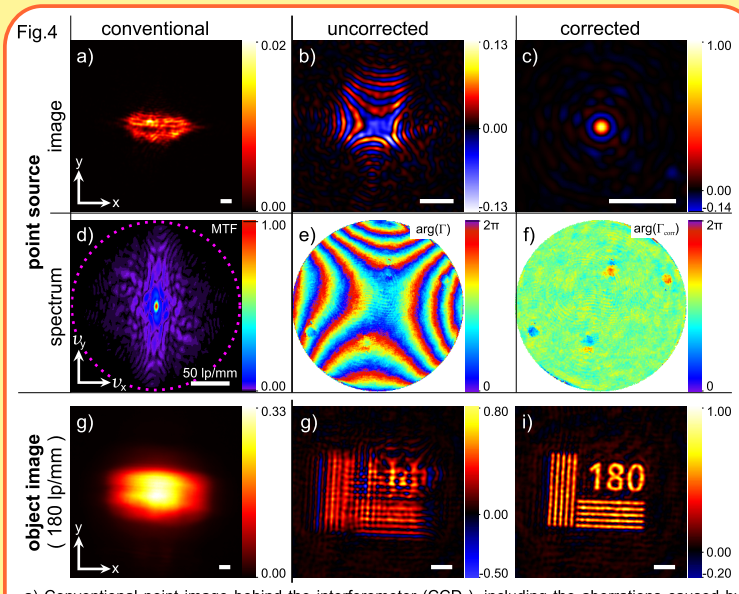

a) Conventional point image behind the interferometer (CCD_2), including the aberrations caused by the adhesive film, the Dove prisms, and the beam splitters. d) By a Fourier transform of a), the conventional modulation transfer function is obtained, showing that the major part of the object information is irreversibly lost. The reconstructions of the point source by means of Γ with and without the aberration correction are shown in b) and c). The strong improvement can also be observed in the phases of the corresponding coherence functions (e&f). The bottom line shows the images of a test chart under the respective conditions. Note that each scale bar represents 20 µm (object space).

Results

Fig.3 shows the determination of the wave front errors as proposed in Fig.2a. Due to a Zernike polynomial fit, a smooth correction function could be obtained. With the help of this function, the reconstructions of extended objects can be corrected.
The effect of such a numerical aberration correction is demonstrated in Fig.4. Here, the influence on the image of a point source and a test chart is shown. The 180 lp/mm grating has a spatial frequency near the cutoff-frequency of the microscope (221 lp/mm). While the conventional images are blurred, the images gained by the proposed method are quasi diffraction limited.

[1] D.Weigel, H. Babovsky, A. Kiessling, and R. Kowarschik, “Widefield microscopy with infinite depth of field and enhanced lateral resolution based on an image inverting interferometer,” Opt. Commun. 342, 102–108 (2015)
[2] D.Weigel, A. Kiessling, and R. Kowarschik, "Verfahren zur hochaufgelösten Messung des komplexen Kohärenzgrades" 114. Jahrestagung der DGaO, 2013, P23
[3] D.Weigel, A. Kiessling, and R. Kowarschik, “Aberration correction in coherence imaging microscopy using an image inverting interferometer,” Manuscript submitted for publication.

DGaO-Proceedings 2015 - http://www.dgao-proceedings.de - ISSN: 1614-8436 - urn:nbn:de:0287-2015-P032-3
submitted: 19.06.2015 published: 21.08.2015